

Arsenite-Induced Alterations of DNA
Photodamage Repair and Apoptosis Following
Solar-Simulation UVR in Mouse Keratinocytes *In*
Vitro

Feng Wu, Fredric J. Burns, Ronghe Zhang, Ahmed N. Uddin,
and Toby G. Rossman

doi:10.1289/ehp.7846 (available at <http://dx.doi.org/>)
Online 15 April 2005



Arsenite-Induced Alterations of DNA Photodamage Repair and Apoptosis Following
Solar-Simulation UVR in Mouse Keratinocytes *In Vitro*

Feng Wu, Fredric J. Burns, Ronghe Zhang, Ahmed. N. Uddin and Toby G. Rossman

NYU School of Medicine

Nelson Institute of Environmental Medicine and NYU Cancer Institute

57 Old Forge Road

Tuxedo, NY 10987

Correspondence to Dr. Fredric J. Burns at the above address.

Voice: 845-731-3551

Fax: 845-351-5476

Email: burns@env.med.nyu.edu

Authors are listed in order of their contributions to the work.

Running Head: Keratinocyte response to arsenite and UVR *in vitro*

Key Words: arsenite, skin cancer, mouse keratinocyte, solar-simulation UVR, photodamage repair, apoptosis

Acknowledgments and Grants: This work was supported by NIEHS grant ES09252 and NASA grant NAG9-1528 and is part of The Nelson Institute of Environmental Medicine and the NYU Cancer Institute programs supported by grant CA16087 from the NCI and a Center Grant (ES00260) from the NIEHS. The authors declare they have no competing financial interests.

Abbreviations: UVR = ultraviolet radiation

CPDs = cyclobutane pyrimidine dimers

6-4PPs = 6-4 photoproducts

TUNEL = terminal deoxynucleotide transferase dUTP nick end labeling

NER = nucleotide excision repair

DPBS = Dulbecco's phosphate-buffered saline

EMEM = Eagle's minimum essential medium

NEAA = non-essential amino acids

FBS = fetal bovine serum

EGF = epidermal growth factor

DMBA=7, 12-dimethylbenz[a]anthracene

ELISA = enzyme-linked immunosorbent assay

OD = optical density

FITC~PBR-1 mAb = FITC-conjugated monoclonal antibody to BrdU

Abstract

Introduction

Materials and methods

Results

Discussion

References

Abstract

Our laboratory has shown that arsenite markedly increased the cancer rate caused by solar-simulation ultraviolet radiation (UVR) in the hairless mouse skin model. The current study investigated how arsenite affected DNA photodamage repair and apoptosis following solar-simulation UVR in the mouse keratinocyte cell-line 291.03C. The keratinocytes were treated with different concentrations of sodium arsenite (0.0, 2.5, 5.0 μM) for 24 h, and then were immediately irradiated with a single dose of 0.30 kJ/m^2 UVR. At 24 h after UVR, DNA photoproducts [cyclobutane pyrimidine dimers (CPDs) and 6-4 photoproducts (6-4PPs)], and apoptosis were measured by using ELISA and two color TUNEL (terminal deoxynucleotide transferase dUTP nick end labeling) assay, respectively. The results showed that arsenite reduced the repair rate of 6-4PPs by about a factor of 2 at 5.0 μM and had no effect at 2.5 μM . UVR-induced apoptosis at 24 h was decreased by 22.64% at 2.5 μM arsenite and by 61.90% at 5.0 μM arsenite. Arsenite decreased the UVR-induced caspase-3/7 activity in parallel with the inhibition of apoptosis. Colony survival assays of the 291.03C cells demonstrate an arsenite LC_{50} of 0.9 μM and a UVR LD_{50} of 0.05 kJ/m^2 . If the present results are applicable *in vivo*, inhibition of UVR-induced apoptosis may contribute to arsenite's enhancement of UVR-induced skin carcinogenesis.

Introduction

Previous studies (Burns et al. 2004; Rossman et al. 2001) showed that arsenite markedly increased the cancer incidence of solar-simulation ultraviolet radiation (UVR) in hairless mice. The relationship between arsenite concentration in drinking water and the yield of squamous cell carcinomas in UVR-exposed mouse skin was linear up to 5 mg/l. UVR is a complete carcinogen that readily induces skin cancer (Zhuang et al. 2000). Although UVR induces a wide range of DNA damage, such as protein-DNA crosslinks, oxidative base damage, single-strand breaks and double-strand breaks (de Gruijl et al. 2001), the major DNA damage is cyclobutane pyrimidine dimers (CPDs) and 6-4 photoproducts (6-4PPs). Both of the latter lesions are repaired by nucleotide excision repair (NER) (Mitchell et al. 1985). Failure to repair CPDs and 6-4PPs leads to the signature mutations containing CC to TT and C to T transitions (Miller 1985; Ziegler et al. 1993) that are common in UVR-induced human skin cancers but not in other epithelial cancers (Brash et al. 1996). UVR can stimulate many signal transduction pathways (Bender et al. 1997), which may contribute to skin cancer progression.

Exposure to arsenite is associated with skin, bladder, lung and probably kidney and liver cancers in humans (Rossman 2003). Studies of human cell lines have demonstrated that arsenite can reduce nucleotide excision repair (NER) capacity by inhibiting the DNA incision step (Hartwig et al. 1997). Inhibition of the ligation step in base excision repair (Li and Rossman 1989) by arsenite has also been reported. Arsenite is known to alter the methylation status of the cell, which affects expression of a variety of genes (Zhao et al. 1997). Arsenite also shows high affinity toward vicinyl sulhydryl groups, including, zinc finger proteins identified as transcription factors and several DNA repair enzymes (Hartwig 2001).

The aim of the present study was to examine how arsenite affected the solar-

simulation UVR-induced apoptosis and photodamage repair in mouse keratinocyte line 291.03C *in vitro*. The results showed that arsenite reduced the repair rate of 6-4PPs by about 50% at 5.0 μ M but not at 2.5 μ M, and inhibited apoptosis in mouse keratinocyte cell-line 291.03C.

Materials and methods

Cell culture: Mouse keratinocyte cell line 291.03C, generously provided by Dr. Molly Kulesz-Martin, was grown in Eagle's minimum essential medium (EMEM, Mediatech Cellgro, Herndon, VA) with non-essential amino acids (NEAA, Cellgro) containing 5% fetal bovine serum (FBS), 1% antibiotic-antimycotic and 10 ng/ml epidermal growth factor (EGF) at 37°C in 5% CO₂. The 291.03C line is a 7,12-dimethylbenz[a]anthracene (DMBA) initiated clone derived from non-transformed 291 cells (Kulesz-Martin et al. 1985), and is an precursor of squamous cell carcinoma, which was selected based on the ability to resist extracellular Ca²⁺-induced terminal differentiation, and has distinctive keratinocyte morphology. The gene expression patterns are substantially similar between the non-transformed cell line 291 and 291.03C. The p53 protein in 291.03C is wild type, even if its function is somewhat compromised (Wang et al. 2002).

Ultraviolet irradiation: The ultraviolet radiation (UVR) source was a bank of four FS20 sunlamps (Westinghouse, Bloomfield, NJ) mounted in parallel 15 cm apart. The UVR intensity was measured (30cm below the source) by a calibrated radiometer/photometer (Model IL1400A, International light inc., Newburyport, MA). According to manufacturer specifications, 85% of the lamp output was in the UVB (290-320nm) range, <1% was in the UVC (200-290 nm) range, 4% was in the UVA (320-400nm) range, and the remainder was in the visible (>400 nm) range.

For assays of photodamage repair, apoptosis and caspase activity, 2×10^6

291.03C keratinocytes were seeded in 100 mm culture dishes, and incubated for 24 h with different concentrations (0.0, 2.5 and 5.0 μM) of sodium arsenite (Sigma, St. Louis, MO) beginning at about 70% of confluence. At 24 h the cells were washed with Dulbecco's phosphate-buffered saline (DPBS) (Sigma, St. Louis, MO) twice and exposed to UVR in the presence of 5ml DPBS.

Colony survival assay: Mouse 291.03C keratinocytes were seeded at a density of 300 cells/60 mm dish in EMEM. After 24 h sodium arsenite was added to the medium from a freshly prepared stock solution to final concentrations of 0.0, 0.05, 0.1, 0.5, 1.0 and 5.0 μM , and the cells were incubated for 7 days followed by fixation in methanol then staining with 0.5% crystal violet in 50% methanol. Colonies were counted and the percentage of survival was determined as the ratio of treated to control $\times 100$. The survival after exposure to solar-simulation UVR was determined similarly at 7 days after single doses of 0.0, 0.05, 0.10, 0.20 and 0.30 kJ/m^2 .

Measurement of CPDs and 6-4PPs in genomic DNA by enzyme-linked immunosorbent assay (ELISA): Genomic DNA was isolated by using the QIAamp Blood Kit (QIAGEN Inc, Valencia, CA). DNA concentrations were calculated from the absorbance at 260 nm measured by a Beckman DU[®] 650 spectrophotometer (Beckman Instruments, Fullerton, CA). The quantities of CPDs and 6-4PPs were determined by ELISA as described (Mori et al. 1991). In brief, Falcon[®] polyvinylchloride flat-bottom 96 well assay plates (Becton Dickinson Labware, Franklin Lakes, NJ) precoated with 1% protamine sulfate (Sigma, St. Louis, MO) were incubated with purified genomic DNA (15 ng for CPD detection and 150 ng for 6-4 PP detection) in PBS at 37°C for 20 h. For CPD detection the TDM-2 antibody was used, and for 6-4 PP detection the 64M-2 antibody was used (both antibodies were generously provided by Dr. Toshio Mori, Nara,

Japan). After adding biotinylated F(ab')₂ goat anti-mouse IgG fragments and streptavidin-peroxidase (Zymed, San Francisco, CA), the optical density (OD) from o-phenylene diamine at 492 nm was measured by using a Bio Assay Reader HTS7000 (Perkin-Elmer Corp, Norwalk, CT). The percentage of the initial number of photoproducts was calculated at various times after UVR exposure by using standard curves obtained from DNA samples irradiated with UVR doses of 0.0, 0.06, 0.12, 0.24 and 0.36 kJ/m².

Measurement of Apoptosis by Flow Cytometry: Apoptosis was detected by using the APO-BRDUtm kit (Phoenix Flow Systems, Inc, San Diego, CA) following the protocol provided by the manufacturer. Briefly, attached cells were harvested by trypsinization and combined with free-floating cells that were harvested by centrifugation. After washing with PBS, the cells were fixed with 1% paraformaldehyde in PBS, followed by fixation with 70% ice cold ethanol overnight. The fixed cells were washed twice with Wash Buffer, and freshly prepared DNA labeling solution (containing TdT and Br-dUTP) was added to the cell pellet and incubated overnight at room temperature. Cells were labeled by FITC-conjugated monoclonal antibody to BrdU (FITC~PBR-1 mAb), washed again, resuspended in staining solution containing propidium iodide and RNase and incubated for 30 min at room temperature, after which cells were immediately analyzed by using a Coulter EPICS XL•MCL flow cytometer. The percentage of R1 (normal cells) R2 (apoptotic cells without loss of DNA), and R3 (hypodiploid cells) was calculated by using EXPO32 Multifile software.

Measurement of caspase-3/7 activity by Apo-one Caspase-3/7 Homogenous Assay: Caspase-3/7 activity was measured by using the Apo-one Homogenous Caspase-3/7 Assay (Promega, Madison, WI) following the protocol provided by the manufacturer. In brief, cells were trypsinized and 20,000 cells/sample were mixed with

the same volume of the Apo-one Homogenous Caspase-3/7 reagent. After incubation at room temperature for 2 h, caspase 3/7 activities were estimated from the fluorescence of each sample at the excitation wavelength of 485 nm and the emission wavelength of 535 nm by using the Bio Assay Reader HTS7000. EMEM mixed with the same volume of Apo-one Homogenous Caspase-3/7 reagent served as a negative control.

Results

Toxicity of arsenite and UVR to 291.03C mouse keratinocytes: Figure 1 shows the effects of arsenite (Figure 1a) and solar-simulation UVR (Figure 1b) on clonal survival of 291.03C mouse keratinocytes. The LD₅₀ of UVR was 0.05 kJ/m². There was no measurable colony survival at UV doses above 0.30 kJ/m². The LC₅₀ of sodium arsenite was 0.9 µM. Arsenite did not show significant lethality below 0.5 µM, and showed nearly 100% lethality above 5.0 µM.

In a previous study (Burns et al. 2004), hairless mice were fed sodium arsenite in drinking water at concentrations ranging from 1.25mg/l (9.6 µM) ~10mg/l (77.0 µM), and solar spectrum UVR exposure was applied to the dorsal skin at 1.0 kJ/m² thrice weekly. The arsenite concentrations and solar UVR dose used in the current *in vitro* study were 2.5 µM, 5 µM, and 0.3 kJ/m², respectively. These 2 arsenite concentrations were estimated to be equivalent to 26% and 52% of the lowest arsenite concentration (1.25mg/l) utilized in the *in vivo* carcinogenesis study.

Arsenite effects on DNA photodamage repair: The two photolesions, CPDs and 6-4PPs, were detected by ELISA. The 6-4PPs were 80% removed by 12 h, while CPDs were not removed more than 10% by 24 h (Figure 2). According to the regression analysis of the data, arsenite showed no significant effect on CPDs repair. The 6-4PPs repair rate after UVR was 11.95%/h, when combined with 2.5 µM or 5.0 µM arsenite,

the 6-4PPs repair rate were 11.3%/h and 6.19%/h respectively. Arsenite slowed the 6-4PPs repair rate by 48% at 5.0 μM , but no difference was detected at 2.5 μM .

Arsenite inhibits UVR-induced apoptosis: Figure 3 shows that at 24 h after UVR alone (0.30 kJ/m^2) the percentage of apoptotic cells was 27.6% (Figure 3d). When UVR-treated cells were incubated in 2.5 μM or 5.0 μM arsenite, the percentage of apoptotic cells decreased to 21.4% (77.36% of UVR-only)(Figure 3e) and 10.5% (38.1% of UVR-only)(Figure 3f), respectively. Untreated control cells showed little apoptotic cells (Figure 3a), while 5.0 μM arsenite-only showed 4.9% apoptotic cells at 48 h after treatment (Figure 3 b) and 8.1% at 60 h (Figure 3c) after treatment. Apoptosis was not detected at 0 h and 14 h after UVR, and was 51.56%, 39.42% and 36.47% at 36 h after UVR, UVR+2.5 μM arsenite, UVR+5 μM arsenite, respectively (data not shown), indicating that the apoptosis is progressing with the time. As shown in Figure 3, the R3 population was 5.28% (UVR alone), 3.71% (UVR+2.5 μM arsenite) and 1.32% (UVR+5.0 μM arsenite) respectively, indicating that apoptosis is more extensive following treatment with UVR alone in comparison to UVR+arsenite.

The caspase-3/7 activities at 24 h after UVR are shown in Figure 4. Arsenite decreased the UVR-induced caspase-3/7 activity to 88.48% at 2.5 μM , and to 58.83% at 5 μM . Arsenite alone did not affect the caspase level significantly. These results are consistent with the results in Figure 3 indicating arsenite inhibited UVR-induced apoptosis (Figure 4).

Discussion

The photoproducts (CPDs and 6-4PPs) produced by UVR may lead to mutations and cancer development if the damage is not removed from the DNA. There are two mechanisms for a cell to remove DNA damage: repairing the DNA damage or inducing

apoptosis. Arsenite indeed increased the mutagenicity of UVB in Chinese hamster V79 cells (Li and Rossman 1991). As reported here mouse keratinocytes didn't repair UVR-induced CPDs efficiently, also arsenite didn't affect the DNA photodamage repair rates significantly. The apoptosis inhibiting activity of arsenite may have converted a greater amount of DNA damage to mutations without substantially affecting DNA repair. If so these findings might help to explain why skin cancer in mice is markedly increased by prolonged exposure to the combination of UVR and dietary arsenite.

Although it has been reported that arsenite inhibits DNA repair in a variety of cell types (Hartwig et al. 1997; Li and Rossman 1989; Yager and Wiencke 1997), the study reported here in a mouse keratinocyte cell line (Figure 2) shows little effect of arsenite on the removal of UVR-induced photoproducts from the genomic DNA except the reduced 6-4PPs repair rate at 5 μ M. In normal human epidermal keratinocytes (NHEK, Cambrex BIO Science Walkersville, MA), 6-4PPs were removed at a rate of 30%/h, while CPDs were removed at a rate of 2%/h after a 0.3 kJ/m² of solar-simulation UVR (data not shown). The mouse 291.03C keratinocyte line exhibited a 6-4PPs removal rate of 13%/h and a CPD removal rate of less than 0.4%/h (Figure 2). The repair rates of mouse keratinocytes was not more than 20% for CPDs and 40% for 6-4PPs that of human keratinocytes.

There are two subpathways of NER: transcription-coupled repair (TCR) and global genomic repair (GGR). TCR refers to the preferential repair of transcribed strands of active genes, and GGR refers to repair anywhere else in the DNA. Many rodent cells have normal TCR which is very important for clonal survival, but are deficient in GGR of CPDs, which is more important for suppressing mutagenesis (Hanawalt 2001). Since the ELISA method employed here detects GGR, these results confirm that mouse keratinocyte line 291.03C performs GGR of DNA photodamage less

efficiently than human keratinocyte.

UVR can trigger apoptosis by damaging the DNA and activating the death receptors on the cell surface (Kulms and Schwarz 2000). Arsenite can induce Fas/FasL dependent apoptosis at higher concentrations ($\geq 5.0 \mu\text{M}$) in primary human keratinocytes (Liao et al. 2004). The results reported here show that $5.0 \mu\text{M}$ arsenite produced a small increase (8%) in apoptosis after 60 h of treatment, while a single 0.30 kJ/m^2 dose of solar-simulation UVR produced 27% apoptosis by 24 h, and 51% by 36 h, indicating that apoptosis increased gradually after exposure to UVR. Paradoxically arsenite at the $5.0 \mu\text{M}$ concentration that produced a small incidence of apoptosis by itself, but it was inhibitory when combined with a strongly apoptotic dose of UVR (Figure 3). The caspase results generally confirmed the apoptosis results obtained by flow cytometry. At 36 h after UVR+ $5.0 \mu\text{M}$ arsenite, apoptosis increased to 37% (30% less than UVR alone), indicating that arsenite delayed the onset of the apoptosis, but did not prevent it completely.

In a previous study (Li JH and Rossman TG. 1991) of Chinese hamster V79 cells, the combination of UVB (0.2 kJ/m^2) and sodium arsenite ($10 \mu\text{M}$ and $15 \mu\text{M}$) increased the mutation rates by 1.65 fold and 2.06 respectively, while survival was decreased to 43% and 11.8% respectively. The inhibition of apoptosis may help to explain the higher mutation rates in the presence of arsenite. In conclusion, arsenite lessened the rate of DNA repair and inhibited apoptosis at 24 h after a single exposure of mouse keratinocyte line 291.03C to 0.3 kJ/m^2 of solar-simulation UVR. The consequences of this delay on mutation rates will be investigated in future studies.

References

Bender K, Blattner C, Knebel A, Iordanov M, Herrlich P, Rahmsdorf HJ. 1997. UV-induced signal transduction [review]. *J Photochem Photobiol B* 37:1-17.

Brash DE, Ziegler A, Jonason AS, Simon JA, Kunala S, Leffell DJ. 1996. Sunlight and sunburn in human skin cancer: p53, apoptosis, and tumor promotion [Review]. *J Investig Dermatol Symp Proc* 1:136-142.

Burns FJ, Uddin AN, Wu F, Nádas A, Rossman TG. 2004. Arsenic-Induced Enhancement of Ultraviolet Radiation Carcinogenesis in Mouse Skin: A Dose-Response Study. *Environ Health Perspect* 112:599-603.

de Gruijl FR, van Kranen HJ, Mullenders LH. 2001. UV-induced DNA damage, repair, mutations and oncogenic pathways in skin cancer [review]. *J Photochem Photobiol B* 63:19-27.

Hanawalt PC. 2001. Revisiting the rodent repairadox. *Environ Mol Mutagen* 38:89-96.

Hartwig A. 2001. Zinc finger proteins as potential targets for toxic metal ions: differential effects on structure and function [Review]. *Antioxid Redox Signal* 3:625-634.

Hartwig A, Groblinghoff UD, Beyersmann D, Natarajan AT, Filon R, Mullenders LH. 1997. Interaction of arsenic (III) with nucleotide excision repair in UV-irradiated human fibroblasts. *Carcinogenesis* 18:399-405.

Kulesz-Martin M, Yoshida MA, Prestine L, Yuspa SH, Bertram JS. 1985. Mouse cell clones for improved quantitation of carcinogen-induced altered differentiation. *Carcinogenesis* 6:1245-1254.

Kulms D and Schwarz T. 2000. Molecular mechanisms of UV-induced apoptosis [review]. *Photodermatol Photoimmunol Photomed* 16:195-201.

Li JH, Rossman TG. 1989. Inhibition of DNA ligase activity by arsenite: a possible mechanism of its comutagenesis. *Mol Toxicol* 2:1-9.

Li JH, Rossman TG. 1991. Comutagenesis of sodium arsenite with ultraviolet radiation in Chinese hamster V79 cells. *Biol met.* 4:197-200

Liao WT, Chang KL, Yu CL, Chen GS, Chang LW, Yu HS. 2004. Arsenic induces human keratinocyte apoptosis by the FAS/FAS ligand pathway, which correlates with alterations in nuclear factor-kappa B and activator protein-1 activity. *J Invest Dermatol* 122:125-129.

Miller JH. 1985. Mutagenic specificity of ultraviolet light. *J Mol Biol* 182:45-65.

Mitchell DL, Haipiek CA, Clarkson JM. 1985. (6-4) Photoproducts are removed from the DNA of UV-irradiated mammalian cells more efficiently than cyclobutane pyrimidine dimers. *Mutat Res* 143:109-112.

Mori T, Nakane M, Hattori T, Matsunaga T, Ihara M, Nikaido O. 1991. Simultaneous establishment of monoclonal antibodies specific for either cyclobutane pyrimidine dimer or (6-4) photoproduct from the same mouse immunized with ultraviolet-irradiated DNA. *Photochem Photobiol* 54:225-232.

Rossman TG. 2003. Mechanism of arsenic carcinogenesis: an integrated approach. *Mut Res* 533:37-65.

Rossman TG, Uddin AN, Burns FJ, Bosland MC. 2001. Arsenite is a cocarcinogen with solar ultraviolet radiation for mouse skin: an animal model for arsenic carcinogenesis. *Toxicol Appl Pharmacol* 176:64-71.

Wang Z, Liu Y, Mori M, Kulesz-Martin M. 2002. Gene expression profiling of initiated epidermal cells with benign or malignant tumor fates. *Carcinogenesis* 23:635-643

Yager JW and Wiencke JK. 1997. Inhibition of poly (ADP-ribose) polymerase by arsenite. *Mutat Res* 386:345-351.

Zhao CQ, Young MR, Diwan BA, Coogan TP, Waalkes MP. 1997. Association of arsenic-induced malignant transformation with DNA hypomethylation and aberrant gene expression. *Proc Natl Acad Sci USA* 94:10907-10912.

Zhuang L, Wang B, Sauder DN. 2000. Molecular mechanism of ultraviolet-induced keratinocyte apoptosis [Review]. *J Interferon Cytokine Res* 20:445-454.

Ziegler A, Leffell DJ, Kunala S, Sharma HW, Gailani M, Simon JA, et al. 1993. Mutation hotspots due to sunlight in the p53 gene of nonmelanoma skin cancers. Proc Natl Acad Sci USA 90:4216-4220.

Figure legends

Figure 1: The effect of sodium arsenite (a) and solar-simulation UVR (b) on colony survival and cell cycle progression (c) of mouse keratinocyte line 291.03C. Each point represents the mean \pm SD (n=3).

Figure 2: The effect of sodium arsenite on the repair of CPDs (a) and 6-4 PPs (b) from genomic DNA in 291.03C cells. The cells were treated with arsenite (2.5 or 5.0 μ M) for 24 h, and then exposed to solar-simulation UVR (0.3 kJ/m²). At different time points post exposure, genomic DNA was isolated, and the photodamage was detected by ELISA. Each point represents mean \pm SD (n=3).

Figure 3: The effect of sodium arsenite on the apoptosis caused by solar-simulation UVR. 291.03C cells were treated with 2.5 and 5.0 μ M arsenite for 24 h and then exposed to 0.3 kJ/m² solar-simulation UVR. Apoptosis was analyzed by flow cytometry using APO-BRDUtm kit as described in "Materials and Methods". R1 = normal cells, R2 = apoptotic cells without loss of DNA, R3 = apoptotic hypodiploid cells. The apoptotic cell population was calculated as R2+R3. Panel a: negative control; panel b: treated with arsenite (5.0 μ M) alone for 48 h; panel c: treated with arsenite (5.0 μ M) alone for 60 h; panel d: 24 h post-UVR; panel e: 24 h post-UVR with arsenite (2.5 μ M) and panel f: 24 h post UVR with arsenite (5.0 μ M) treatment. Data shown are mean \pm SD (n=3).

Figure 4: The effect of sodium arsenite on caspase-3/7 activity. 291.03C cells were treated with 2.5 and 5.0 μ M arsenite for 24 h and then exposed to 0.3 kJ/m² solar-simulation UVR. Twenty-four hours post UVR, caspase-3/7 activity was measured by

using the Apo-ONE Homogenous Caspase-3/7 Assay. The data shows a close parallel with the apoptosis data from Figure 3. Data are the means \pm SD (n=3).

Figure 1

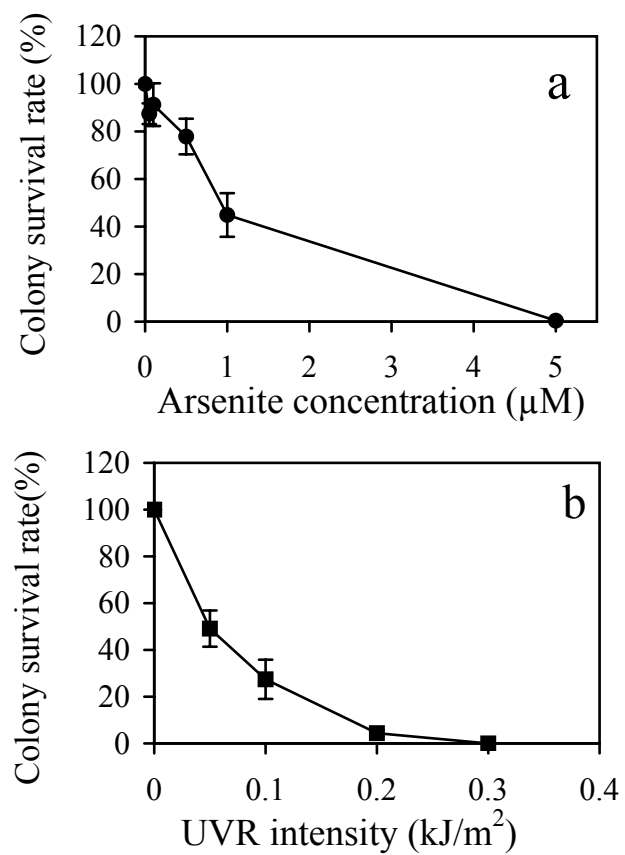


Figure 2

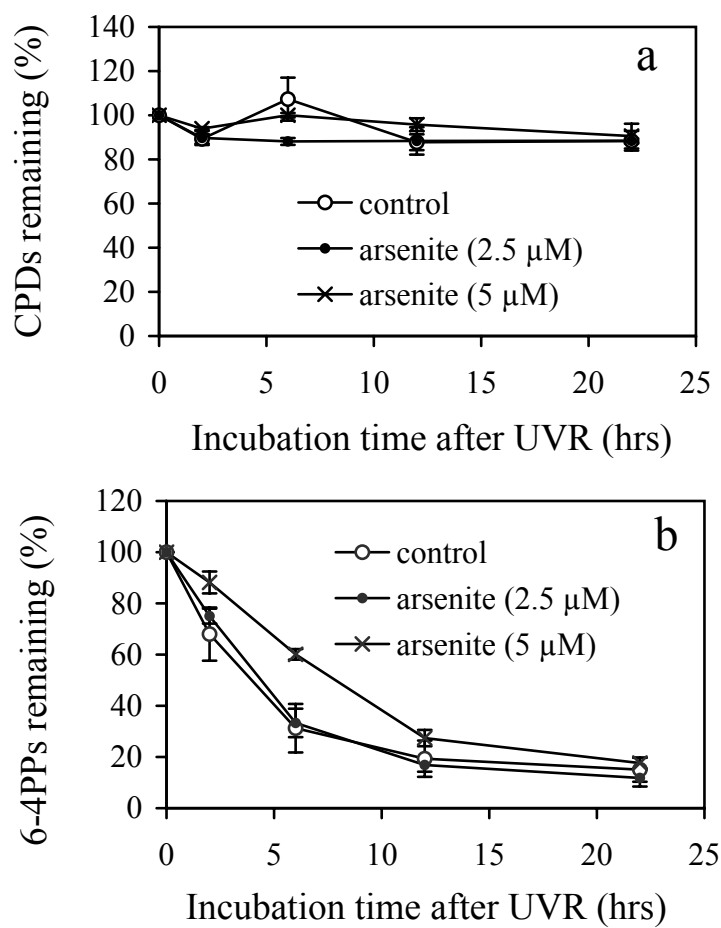


Figure 3

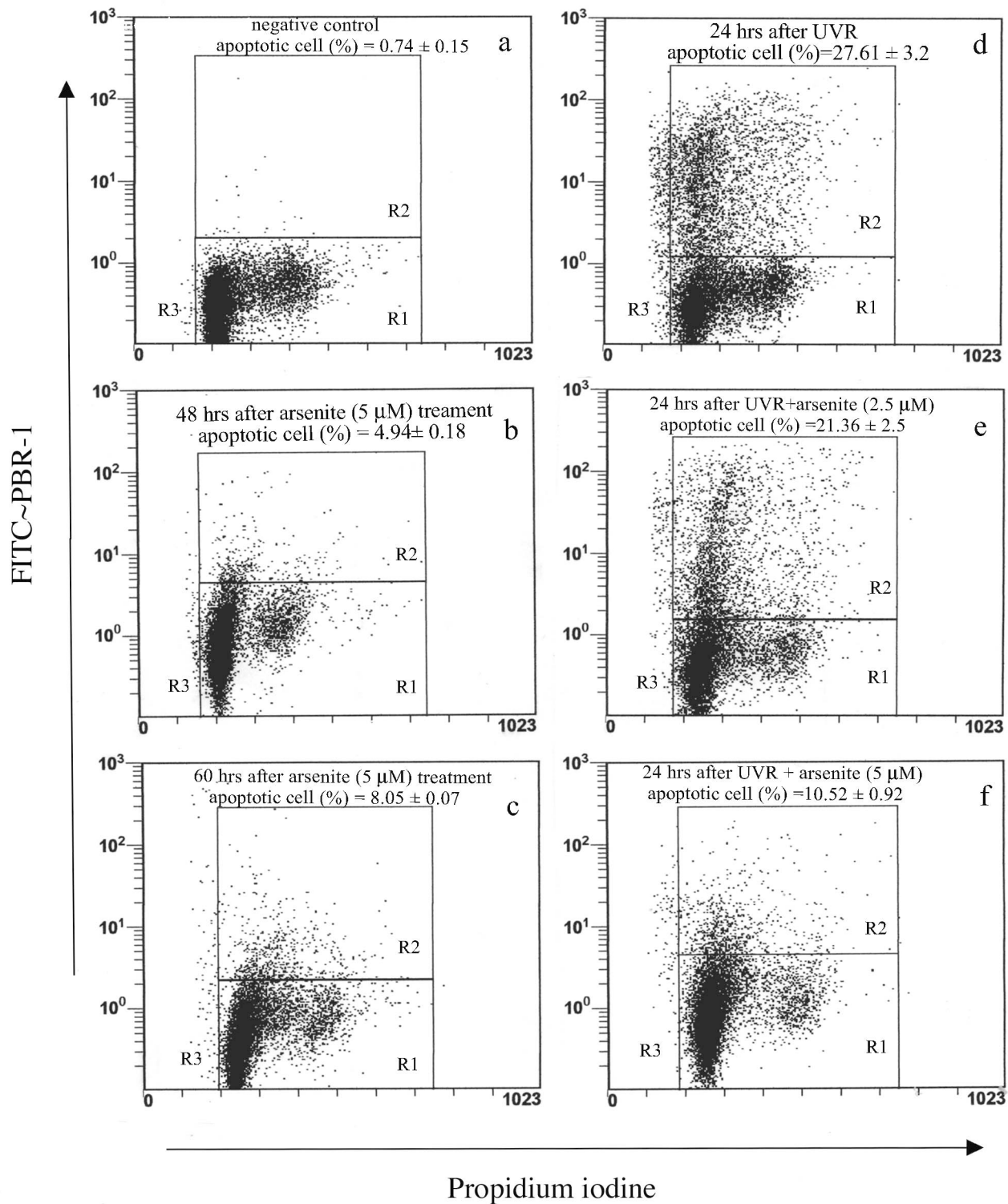


Figure 4

	<i>Apoptosis (%)</i>	<i>Caspase (%)</i>
UVR	100	100
UVR+arsenite (2.5 μ M)	77.36	88.48
UVR+arsenite (5 μ M)	38.1	58.83
arsenite (5 μ M)	17.89	21.01
without treatment	2.68	17.64

